

Article

Surface Segregation of Amphiphilic PDMS-Based Films Containing Terpolymers with Siloxane, Fluorinated and Ethoxylated Side Chains

Elisa Martinelli ¹, Elisa Guazzelli ¹ , Antonella Glisenti ² and Giancarlo Galli ^{1,*}

¹ Dipartimento di Chimica e Chimica Industriale and UDR Pisa INSTM, Università di Pisa, 56124 Pisa, Italy; elisa.martinelli@unipi.it (E.M.); elisa.guazzelli@hotmail.it (E.G.)

² Dipartimento di Scienze Chimiche, Università di Padova, 35131 Padova, Italy; antonella.glisenti@unipd.it

* Correspondence: giancarlo.galli@unipi.it; Tel.: +39-050-2219-272

Received: 29 January 2019; Accepted: 25 February 2019; Published: 26 February 2019



Abstract: (Meth)acrylic terpolymers carrying siloxane (Si), fluoroalkyl (F) and ethoxylated (EG) side chains were synthesized with comparable molar compositions and different lengths of the Si and EG side chains, while the length of the fluorinated side chain was kept constant. Such terpolymers were used as surface-active modifiers of polydimethylsiloxane (PDMS)-based films with a loading of 4 wt%. The surface chemical compositions of both the films and the pristine terpolymers were determined by angle-resolved X-ray photoelectron spectroscopy (AR-XPS) at different photoemission angles. The terpolymer was effectively segregated to the polymer–air interface of the films independent of the length of the constituent side chains. However, the specific details of the film surface modification depended upon the chemical structure of the terpolymer itself. The exceptionally high enrichment in F chains at the surface caused the accumulation of EG chains at the surface as well. The response of the films to the water environment was also proven to strictly depend on the type of terpolymer contained. While terpolymers with shorter EG chains appeared not to be affected by immersion in water for seven days, those containing longer EG chains underwent a massive surface reconstruction.

Keywords: surface-active polymer; surface segregation; surface modification; amphiphilic polymer; polysiloxane; fluoropolymer; PEGylated polymer; X-ray photoelectron spectroscopy

1. Introduction

The dispersion of non-reactive surface-active additives is generally regarded as a facile and straightforward method to modify the surface properties of a polymer film without affecting its bulk properties to a significant extent [1–4]. The surface segregation process and, therefore, the selective accumulation of the additive at the interface with the external environment (air, water, organic vapors) is a complex phenomenon that depends on several factors that may add to each other, including the additive molecular structure and composition, molecular weight, surface tension, chemical compatibility with the host matrix and chemical affinity with the external environment [5–10]. A special class of surface-active additives consists of amphiphilic copolymers [11–13]. Random copolymers in particular have gained a great deal of interest in the last decade being their synthesis easier and more suitable for an industrial scale production than the block copolymer counterparts [14]. Notably, random copolymers have been proven to generate nanostructured materials as a result of their self-assembling in solution [15–20], bulk and at the surface of polymer thin films [4,21]. In the field of coatings, surface-active additives have been utilized for several purposes, especially for the development of antifouling (AF)/fouling-release (FR) coatings to combat marine biofouling [12]. In this regard, reactive [22–25] and non-reactive amphiphilic copolymers [21,26–29] generally composed

of poly(ethylene glycol) (PEG) chains, as the hydrophilic component, and polysiloxane and/or fluoropolymer chains, as the hydrophobic component, have been investigated. The hydrophilic component of election is PEG on the basis of its known high resistance to the adhesion of proteins, bacteria, cells and marine organisms [30,31]. Moreover, fluorinated and siloxane chains, besides performing a FR action attributed to their hydrophobicity [32,33], can also play other distinct roles. In particular, fluorinated chains are anticipated to promote the diffusion and accumulation of the entire copolymer to the coating surface, as a result of their ability to self-segregate and self-organize at the outermost surface layers of polymer films [34–36]. Polysiloxane chains are also known to have a low surface tension behavior, albeit this character is not so distinct as for fluorinated chains [37–39], and have been introduced into several types and architectures of polymers to modify the surface properties [40,41]. However, in this case, the main role of polysiloxane chains is to act as a compatibilizer with the host elastomeric polydimethylsiloxane (PDMS) matrix to prevent macrophase separation. Moreover, low modulus PDMS-based films are generally thought to favor removal of marine organisms by a peeling-like, lower-energy mechanism [33,42].

In this work, we prepared novel amphiphilic films composed of a condensation-cured PDMS matrix, in which an opportunely designed surface-active amphiphilic terpolymer was physically dispersed in order to modify the surface structure and property of the films derived therefrom. The synthesized terpolymers, consisting of a (meth)acrylic backbone carrying fluorinated (F), ethoxylated (EG) and siloxane (Si) side chains, possessed comparable mole percentages of each type of side chains, but different lengths of the EG and Si and chains, while the length of the F chain was fixed. In particular, we studied the surface nanoscale composition and surface segregation of the terpolymer by means of angle-resolved X-ray photoelectron spectroscopy (AR-XPS). Interestingly, we found that the chemical composition of the PDMS-based films within the first few nanometers (~3 nm) of the surface was almost equal to that of the corresponding pristine terpolymer included in the formulation, independent of its chemical structure. However, the amount of each element at the surface as well as the effectiveness of surface segregation were strongly affected by the structure of the terpolymer itself. A peculiar reconstruction of the film surface was found when the PDMS-based films were immersed in water, which unexpectedly did not result in an increased concentration of the hydrophilic EG chains at the outer surface to contact water.

2. Materials and Methods

2.1. Materials

1H,1H,2H,2H-perfluorooctyl acrylate (F) (Fluorochem, 97%), polyethyleneglycol methyl ether methacrylate (EGa ($M_n = 300 \text{ g mol}^{-1}$) and EGb ($M_n = 1100 \text{ g mol}^{-1}$)), bismuth neodecanoate (BiND) (all from Aldrich), monomethacryloxypropyl-terminated poly(dimethyl siloxane) (Sia ($M_n = 1000 \text{ g mol}^{-1}$) and Sib ($M_n = 5000 \text{ g mol}^{-1}$)), bis(silanol)-terminated poly(dimethyl siloxane) (HO-PDMS-OH ($M_n = 26,000 \text{ g mol}^{-1}$, 0.1% OH)), poly(diethoxy siloxane) (ES40) (all from ABCR) were used as received. 2,2'-azobis-isobutyronitrile (AIBN) (from Fluka) was recrystallized from methanol. Diethylene glycol dimethyl ether (diglyme) was kept at 100 °C over sodium for 4 h and then distilled under reduced pressure.

2.2. General Procedure for the Preparation of Terpolymers

In a typical preparation of a terpolymer p(Sib-F-EGb), monomers Sib (3.400 g, 0.68 mmol), F (0.860 g, 2.05 mmol) and EGb (0.780 g, 0.71 mmol), free-radical initiator AIBN (53.7 mg) and anhydrous solvent diglyme (20 mL) were introduced into a Carius tube. The solution was outgassed by four freeze-pump-thaw cycles. The polymerization reaction was let to proceed under stirring at 65 °C for 72 h. The crude product was purified by several precipitations from chloroform solutions into methanol (yield 48%). The obtained terpolymer p(Sib-F-EGb) contained 26 mol% Sib, 45 mol% F and 29 mol% EGb ($M_n = 21000 \text{ g mol}^{-1}$, $M_w/M_n = 2.2$).

^1H -nuclear magnetic resonance (NMR) (CDCl_3): δ (ppm) = 4.6–3.8 (COOCH_2), 3.8–3.5 (CH_2O), 3.4 (OCH_3), 2.5 (CF_2CH_2), 2.1–0.7 (CH_2CCH_3 , CH_2CH , $\text{COOCH}_2\text{CH}_2\text{CH}_2\text{Si}$, $\text{SiCH}_2\text{CH}_2\text{CH}_2\text{CH}_3$), 0.5 (SiCH_2), 0.1 (SiCH_3).

^{19}F -NMR ($\text{CDCl}_3/\text{CF}_3\text{COOH}$): δ (ppm) = -5.5 (CF_3), -38.5 (CF_2CH_2), -46 to -48 (CF_2), -51 (CF_2CF_3).

Fourier transform-infrared (FT-IR) (film): (cm^{-1}) = 2963–2906 (ν C–H aliphatic), 1738 (ν C=O ester), 1260 and 799 (ν Si– CH_3), 1207–1020 (ν C–F, ν C–O, ν Si–O), 662 (ω CF_2).

2.3. Preparation of Films

Glass slides ($76 \times 26 \text{ mm}^2$) were rinsed with acetone and dried in an oven for 30 min. A solution of HO-PDMS-OH (5.0 g), ES40 (0.125 g) and BiND (50 mg) in ethyl acetate (25 mL) was spray-coated onto the glass slides using a Badger model 250 airbrush (50 psi air pressure). The films were dried at room temperature for a day and annealed at 120°C for 12 h to form a thin bottom layer (thickness $\sim 2 \mu\text{m}$). On top of it, a solution of the same amounts of HO-PDMS-OH, ES40 and BiND with a terpolymer p(Si-F-EG) (200 mg) in ethyl acetate (20 mL) was cast and cured at room temperature for a day and later at 120°C for 12 h to give a thicker top layer (overall thickness $\sim 200 \mu\text{m}$). The blend films containing 4 wt% terpolymer (with respect to the PDMS matrix) in the top layer were named p(Si-F-EG)4. A film of PDMS alone was also prepared in the same way as a standard film.

Films of the pristine terpolymers were prepared by spin-coating (5000 rpm for 20 s) a filtered 3 wt% solution in chloroform and dried at room temperature for 12 h and then at 120°C for 12 h (thickness $\sim 200 \text{ nm}$).

2.4. Characterization

^1H -NMR and ^{19}F -NMR spectra were recorded with a Varian Gemini VRX300 spectrometer (Palo Alto, CA, USA) on CDCl_3 and $\text{CDCl}_3/\text{CF}_3\text{COOH}$ solutions, respectively. Gel permeation chromatography (GPC) analyses were carried out using a Jasco PU-1580 liquid refractive index detector (Hachioji-shi, Tokyo, Japan). CHCl_3 was used as an eluent with a flow rate of 1 mL min^{-1} and poly(methyl methacrylate) standards were used for calibration.

Differential scanning calorimetry (DSC) analysis was performed with a Mettler DSC-30 instrument (Columbus, OH, USA) from -150 to 80°C at heating/cooling rate of $10^\circ\text{C min}^{-1}$ under a dry nitrogen flow. The glass transition temperature (T_g) was taken as the inflection temperature in the second heating cycle.

Contact angles were measured by the sessile droplet ($10 \mu\text{L}$) method with a FTA200 Camtel goniometer (Portsmouth, VA, USA), using water (θ_w) (J. T. Baker, HPLC grade) as wetting liquid after 10 s from deposition.

Atomic force microscopy (AFM) experiments under ambient conditions were carried out in intermittent contact (tapping) mode with a Multimode system equipped with a Nanoscope IIIa controller (Veeco Instruments, New York, USA) using silicon cantilevers with a nominal force constant of 42 N m^{-1} from Olympus type OMCL-AC160TS (Tokyo, Japan) at a resonance frequency of about 320 kHz. The scan rate was kept at 1 Hz, while the tip-sample forces were carefully minimized to avoid artifacts. Tip radius of less than 7 nm (manufacturer's information) was used. To quantify the variation in the microscale structure of the coatings, the root-mean-square roughness (RMS) was determined over regions of $1 \times 1 \mu\text{m}^2$ and $10 \times 10 \mu\text{m}^2$:

$$\text{RMS} = \sqrt{\frac{1}{m n} \sum_{j=1}^n \sum_{i=1}^m Z^2(x_i, y_j)} \quad (1)$$

with Z the height and x, y the in-plane coordinates stored by the AFM software (version 6.13).

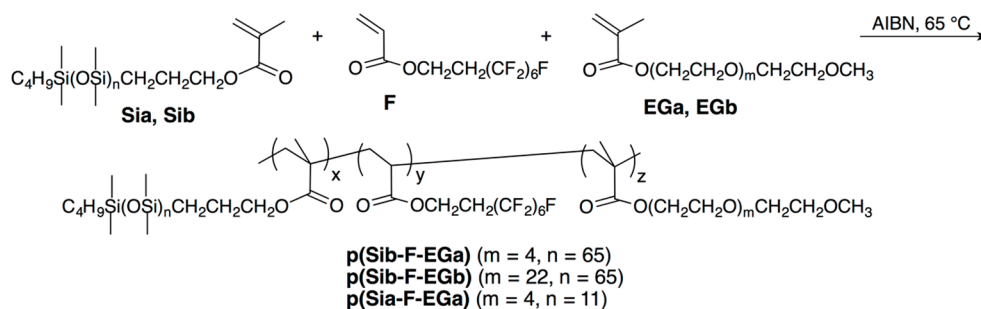
X-ray photoelectron spectroscopy (XPS) spectra were recorded by using a Perkin-Elmer PHI 5600 spectrometer (Chanhassen, MN, USA) with a standard Al-K α source (1486.6 eV) operating at

300 W. The working pressure was less than 10^{-8} Pa. The spectrometer was calibrated by assuming the binding energy (BE) of the Au $4f_{7/2}$ line to be 84.0 eV with respect to the Fermi level. Extended (survey) spectra were collected in the range 0–1350 eV (187.85 eV pass energy, 0.4 eV step, 0.05 s step^{-1}). Detailed spectra were recorded for the following regions: C(1s), O(1s), Si(2p) and F(1s) (11.75 eV pass energy, 0.1 eV step, 0.1 s step^{-1}). The standard deviation (SD) in the BE values of the XPS line was 0.1 eV. The spectra were recorded at two photoemission angles φ (between the surface normal and the path taken by the photoelectrons) of 70° and 20° , corresponding to sampling depths d of $\sim 3 \text{ nm}$ and $\sim 9 \text{ nm}$, respectively ($d = d_0 \cos \varphi$, where d_0 is the maximum information depth ($d_0 \sim 10 \text{ nm}$ for the C(1s) line)). The software used for background subtraction (Shirley type) [43] and quantitative analysis was the PHI software (version 5.2) for data collection in PHI 5600ci Multitechnique (Chanhassen, MN, USA). The atomic percentage was evaluated using the PHI sensitivity factors (considering both the cross-section and the beam out depth) with triplicate measurements on different film spots and the estimated experimental error was $\pm 0.5\%$ [44]. To take into account charging problems, the C(1s) peak was considered at 284.5 eV and the peak BE differences were evaluated. The XPS peak fitting procedure was carried out by means of Voigt functions and the results evaluated through the χ^2 function [45]. The deconvolution of XPS signals was performed with the software Igor Pro.

3. Results and Discussion

3.1. Synthesis of Terpolymers

Amphiphilic terpolymers p(Si-F-EG) with siloxane, fluorinated and ethoxylated side chains were prepared by free-radical polymerization of monomethacryloxypropyl-terminated poly(dimethyl siloxane) (Si), 1H,1H,2H,2H-perfluorooctyl acrylate (F) and polyethyleneglycol methyl ether methacrylate (EG). The terpolymers were characterized by a similar molar content of the three co-units, but differed in the average lengths, i.e. the average number degrees of polymerization of the EG and Si side chains, $m \sim 4$ (EGa) and $m \sim 22$ (EGb) and $n \sim 11$ (Sia) and $n \sim 65$ (Sib), while that of the F side chain was fixed (6 CF_2 groups) (Scheme 1). The formation of terpolymers was confirmed by $^1\text{H-NMR}$, $^{19}\text{F-NMR}$ and FT-IR analyses. Their chemical composition was evaluated from the integrated areas of the signals at 0.5 ppm (SiCH_2 of Sia and Sib), 2.5 ppm (CH_2CF_2 of F) and 3.3 ppm (OCH_3 of EGa and EGb). Therefore, by alternatively changing the length of the siloxane and ethoxylated chains it was possible to modify the content of hydrophobic/hydrophilic co-units, that is the amphiphilic character, of the surface-active terpolymer and the eventual ability of the film surface to interact/reconstruct after immersion in water.



Scheme 1. Synthesis of amphiphilic terpolymers p(Si-F-EG) consisting of x , y , and z mol% co-units carrying Si, F, and EG side chains, respectively.

The thermal behavior of the terpolymers strictly depended on the type of the constituent co-units (Table 1). In particular, p(Sia-F-EGa) was completely amorphous and showed two glass transition temperatures (T_g) at -124°C and -52°C similar to those of the corresponding homopolymers p(Sia) and p(EGa), respectively. Differently, p(Sib-F-EGb) showed two melting transitions at -53°C and 21°C due to the longer Sib and EGb side chains, respectively, in addition to a T_g at -129°C typical

of the siloxane chain. The T_g of the EGb, expected at ca. -60 °C, was not detected because it was superimposed to the melting peak of the Sib (Figure S1). p(Sib-F-EGa) displayed an intermediate behavior showing only the two thermal transitions of the longer polysiloxane Sib, while the T_g of the shorter EGa was hidden by the melting peak of the Sib. These results indicate that all the terpolymers were microphase separated in the bulk in EG-rich and Si-rich domains, each of which displayed the thermal behavior of the respective homopolymer.

Table 1. Physical-chemical properties of terpolymers p(Si-F-EG).

Terpolymer	Composition ^{a)} (mol%)	M_n ^{b)} (g/mol)	M_w/M_n ^{b)}	$T_{g,Si}$ ^{c)} (°C)	$T_{g,EG}$ ^{c)} (°C)	$T_{m,Si}$ ^{c)} (°C)	$T_{m,EG}$ ^{c)} (°C)
p(Sib-F-EGb)	26/45/29	21000	2.22	-129	-	-53	21
p(Sib-F-EGa)	22/52/26	21000	2.06	-129	-	-54	-
p(Sia-F-EGa)	19/58/23	9000	2.94	-124	-52	-	-

^{a)} Mole percentage of siloxane (Si), fluorinated (F) and ethoxylated (EG) side chains in the terpolymer. ^{b)} By gel permeation chromatography (GPC). ^{c)} Glass transition temperature and melting temperature of Si and EG.

The amphiphilic terpolymers were used as non-reactive, physically dispersed surface-active additives in condensation cured PDMS matrices. The terpolymers were dissolved in ethyl acetate together with the bis(silanol)-terminated PDMS matrix and the ES40 cross-linker, in the presence of bismuth neodecanoate as catalyst. The solution was cast on glass slides, previously modified by deposition of a thin layer (~ 2 μm) of cross-linked PDMS. This bottom thinner layer acted as a primer to improve adhesion between the glass substrate and the film formulation (overall thickness ~ 200 μm) to avoid delamination of the film during the subsequent tests upon immersion in water.

Each terpolymers were dispersed in a 4 wt% content with respect to the PDMS matrix in the top layer and the corresponding films were named p(Si-F-EG)4.

3.2. Surface Segregation of the Amphiphilic Surface-Active Terpolymer

Surface segregation of the terpolymer in the condensation-cured matrix films was investigated by AR-XPS at photoemission angles φ of 70° and 20° . The survey spectra of the samples did not show the presence of elements other than Si, C, O, and F (Figure 1). The XPS atomic surface compositions of the films p(Si-F-EG)4 are reported in Table 2 together with those of the respective terpolymers. For comparison, the calculated theoretical values for ideal homogeneous samples are also added in Table 2.

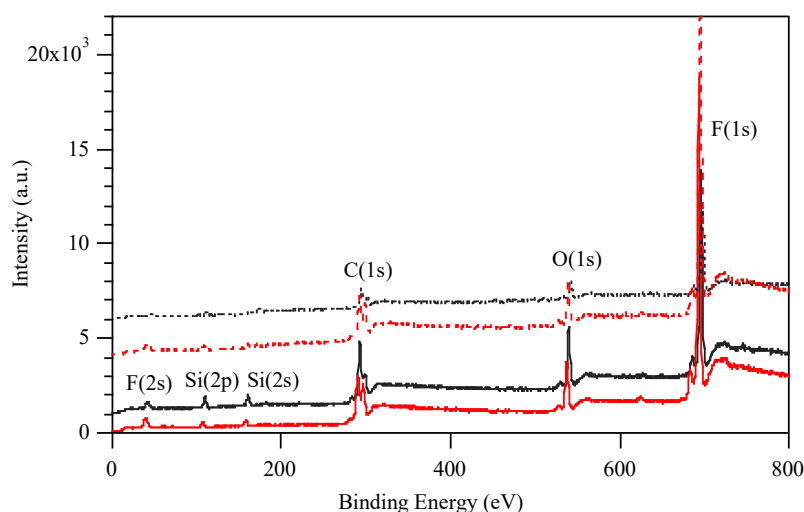


Figure 1. X-ray photoelectron spectroscopy (XPS) survey spectra for the amphiphilic polydimethylsiloxane (PDMS)-based film p(Sia-F-EGa)4 (dashed line) and the respective terpolymer p(Sia-F-EGa) (continuous line) at φ of 70° (red) and 20° (black).

Table 2. XPS atomic surface composition of amphiphilic PDMS-based films p(Si-F-EG)4 and respective terpolymers p(Si-F-EG). The errors on the values of composition were estimated to be $\pm 0.5\%$.

Film	φ (°)	C (%)	O (%)	F (%)	Si (%)	C_{exp}/C_{theor}	O_{exp}/O_{theor}	F_{exp}/F_{theor}	Si_{exp}/Si_{theor}
p(Sib-F-EGa)	theor.	51.4	22.0	8.4	18.2				
	70	42.2	13.4	37.7	6.7	0.8	0.6	4.5	0.4
	20	45.2	20.3	20.5	14.0	0.9	0.9	2.4	0.8
p(Sib-F-EGb)	theor.	54.0	24.2	5.5	16.3				
	70	44.7	17.1	29.9	8.3	0.8	0.7	5.4	0.5
	20	47.0	22.3	17.3	13.4	0.9	0.9	3.1	0.8
p(Sia-F-EGa)	theor.	52.3	16.6	23.9	7.2				
	70	43.5	10.0	44.1	2.4	0.8	0.6	1.8	0.3
	20	45.7	14.3	34.8	5.2	0.9	0.9	1.5	0.7
p(Sib-F-EGa)4	theor.	50.0	24.9	~0.4	24.7				
	70	41.1	11.2	43.0	4.7	0.8	0.4	107.5	0.2
	20	45.9	18.8	23.3	12.0	0.9	0.8	58.3	0.5
p(Sib-F-EGb)4	theor.	50.2	25.0	~0.2	24.6				
	70	42.8	15.8	34.2	7.2	0.9	0.6	171.0	0.3
	20	48.0	22.7	16.8	12.5	1.0	0.9	84.0	0.5
p(Sia-F-EGa)4	theor.	50.1	24.6	1.1	24.2				
	70	42.6	10.1	45.4	1.9	0.8	0.4	41.2	0.1
	20	46.3	12.3	37.9	3.5	0.9	0.5	34.4	0.1

All the pristine terpolymer films showed a high enrichment in fluorine at the surface, the fluorine atomic percentage (F_{exp}) being higher than the theoretical value (F_{theor}) for all the samples. However, while F_{exp} was higher for p(Sia-F-EGa) with a larger F_{theor} , the F_{exp}/F_{theor} ratio was found to decrease from 5.4 and 4.5 down to 1.8 in going from p(Sib-F-EGb) and p(Sib-F-EGa) to p(Sia-F-EGa) ($\varphi = 70^\circ$). Thus, a longer siloxane chain (Sib, $n \sim 65$) promoted a more effective surface segregation of the terpolymer than a shorter one (Sia, $n \sim 11$). Consistently, the Si_{exp}/Si_{theor} ratio followed the same trend, passing from 0.5 and 0.4 down to 0.3. Because of the great enrichment in fluorine in the top few nanometers, the atomic percentages of all the other elements C, O and Si were significantly lower than the theoretical ones. Moreover, the atomic percentages varied with φ . In particular, the F percentage markedly increased, whereas the C, O and Si percentages decreased with increasing φ . Thus, there was a composition gradient along the normal to the film surface into the bulk.

It was surprising that the surface chemical composition of the PDMS-based films containing 4 wt% terpolymer did not differ significantly from that of the respective pristine terpolymer and the F_{exp} was even slightly higher for all the PDMS-based films, despite the fact that PDMS was the largely major component (96 wt%) in all formulations. Thus, neither the thickness of the film nor the presence of the PDMS matrix affected the surface migration of the fluorinated side chains to a significant extent. Similar findings were reported for hydrophobic, i.e. not amphiphilic, (meth)acrylic copolymers containing siloxane and fluorinated side chains, for which a very effective surface segregation was found [9,46]. The observed surface enhancement in fluorine content resulted in an exceptionally high value of F_{exp}/F_{theor} , varying from 41.2 for p(Sia-F-EGa), to 107.5 for p(Sib-F-EGa) up to 171.0 for p(Sib-F-EGb). Accordingly, a strong decrease in Si_{exp} was also observed for all the films, and in particular for p(Sia-F-EGa)4 with the higher amount of fluorine at the surface and the shorter siloxane chains.

The C(1s) high resolution spectra for the PDMS-based films and the terpolymers are shown in Figure 2. In all cases the C(1s) signal was resolved in five contributions, as is shown for p(Sib-F-EGa)4, as a representative illustration, in Figure 3: (i) C–C and C–Si at 284.5 eV, (ii) C–O at 286.1 eV, (iii) C(=O)O at 289.1 eV, (iv) CF_2 at 291.7 eV and (v) CF_3 at 294.1 eV. From a qualitative point of view, the most striking finding was that the individual components of the C(1s) spectra of the blend films almost fully overlapped those of the respective terpolymers. This finding demonstrates that the amphiphilic terpolymer was completely located to the polymer–air interface of the PDMS-based films, independent of the length of the EG or Si chains, and the structural arrangement of each constituent at the molecular level was basically the same for the terpolymer whether alone or in the blend. Although the peaks (ii) to (v) had almost the same intensities in the blends and respective

terpolymers, a decrease in the intensity of peak (i) was observed, especially for the formulations containing p(Sib-F-EGa) and p(Sib-F-EGb), which is in agreement with a better segregation of the F side chains to the topmost surface layers for these terpolymers, as already suggested by the $F_{\text{exp}}/F_{\text{theo}}$ ratio (Table 3). Finally, one notes that the contribution due to C–O groups of the EG side chains was also remarkably higher for all the films than the theoretical value calculated for the respective terpolymers (Table 3). Thus, the EG side chains, in spite of their high surface energy, were pulled to the outer surface by the lowest surface energy F side chains. In particular, films with the shorter Ea chains displayed a larger surface enrichment in C–O groups (peak (ii), $C-O_{\text{exp}}/C-O_{\text{theo}} \sim 5$ and ~ 3 for p(Sib-F-EGa) and p(Sia-F-EGa), respectively) with respect to films containing EGb ($C-O_{\text{exp}}/C-O_{\text{theo}} \sim 1.3$), owing to the higher mobility of the shorter EGa chains. The dependence of the surface segregation of the EG chains on their chain length was also confirmed by the fact that the C–O percentage at $\varphi = 70^\circ$ was higher than that at $\varphi = 20^\circ$ for the films containing EGa and lower for those containing EGb (Table 3). Therefore, for copolymers containing EGa side chains the concentration of the EG chains within the outer ~ 3 nm of the polymer–air interface was maximized, in spite of their high surface energy ($\sim 43 \text{ mN m}^{-1}$). On the other hand, the intensity of the peak associated with the Si–C contribution markedly increased, while that of the CF_2 signal significantly decreased and that of the CF_3 signal completely disappeared in some cases (Figure S2).

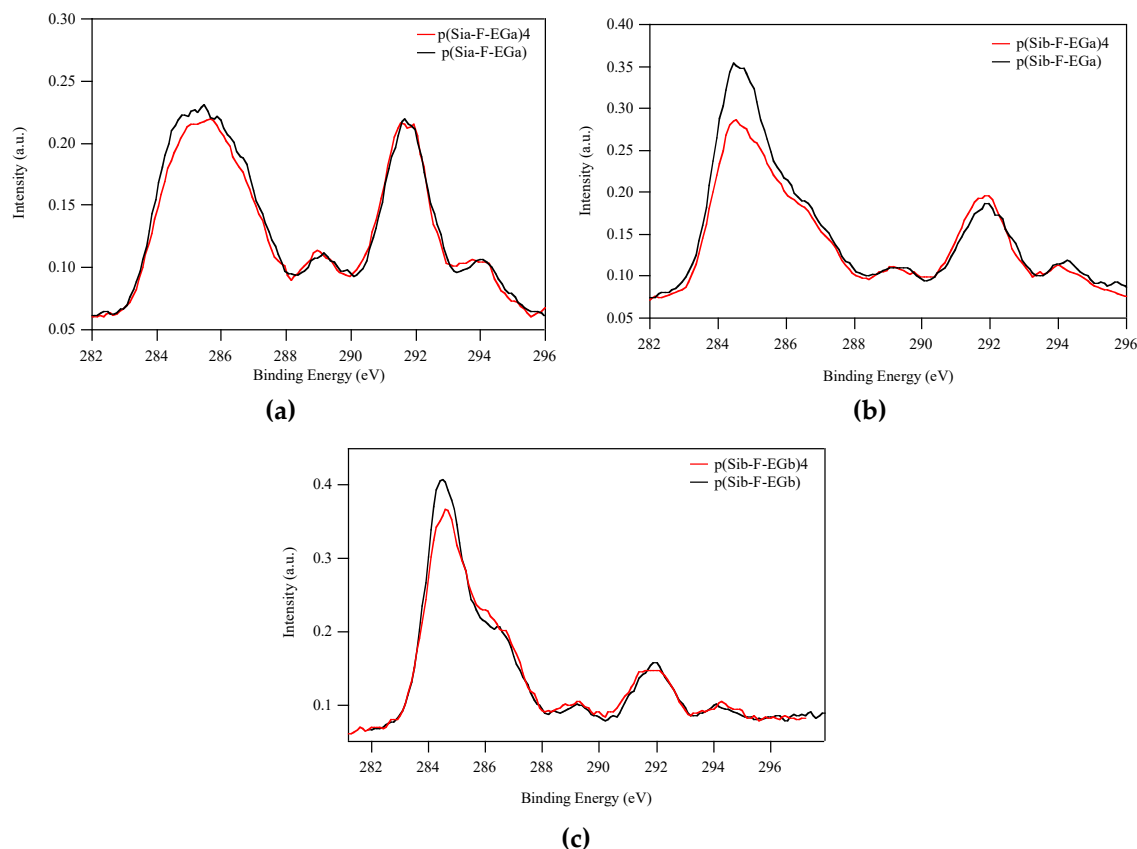


Figure 2. Area-normalized XPS C(1s) spectra ($\varphi = 70^\circ$) for the amphiphilic PDMS-based films p(Si-F-EG)4 (red) and the respective terpolymers p(Si-F-EG) (black). (a) p(Sia-F-EGa)4 and p(Sia-F-EGa); (b) p(Sib-F-EGa)4 and p(Sib-F-EGa); (c) p(Sib-F-EGb)4 and p(Sib-F-EGb).

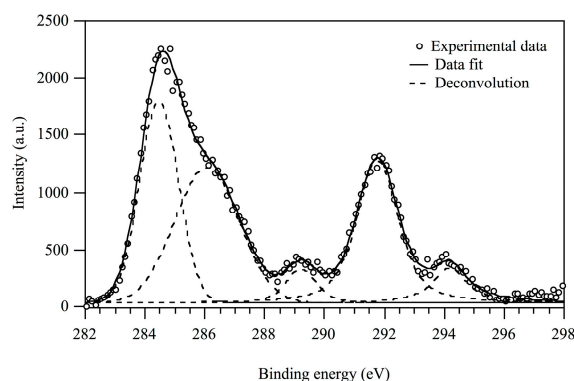


Figure 3. Deconvolution of the C(1s) XPS spectrum of p(Sib-F-EGa)4 ($\varphi = 70^\circ$).

Table 3. Percent contributions of peaks (i)–(v) to the XPS C(1s) signal for the amphiphilic PDMS-based films p(Si-F-EG)4.

Film	φ (°)	Peak (i) (%)	Peak (ii) (%)	Peak (iii) (%)	Peak (iv) (%)	Peak (v) (%)
p(Sib-F-EGa)4 ^{a,b}	70	29.1	32.3	4.8	27.2	6.6
	20	61.0	24.3	3.5	11.2	-
p(Sib-F-EGb)4 ^{a,b}	70	44.5	32.0	4.4	14.4	4.7
	20	50.6	38.3	2.6	8.5	-
p(Sia-F-EGa)4 ^{a,b}	70	14.6	38.0	6.0	34.7	6.7
	20	35.0	27.6	9.1	23.3	5.0

^{a)} Experimental percent contributions of peaks (i)–(v) for terpolymers p(Sib-F-EGa): 37.5%, 35.2%, 4.2%, 17.6%, 5.5%; p(Sib-F-EGb): 49.8%, 31.4%, 3.2%, 12.5%, 3.1%; p(Sia-F-EGa): 16.2%, 40.1%, 5.3%, 32.1%, 6.3%. ^{b)} Theoretical percent contributions of peaks (i)–(v) for terpolymers p(Sib-F-EGa): 80.0%, 10.0%, 2.4%, 6.3%, 1.3%; p(Sib-F-EGb): 67.5%, 26.0%, 1.8%, 3.9%, 0.8%; p(Sia-F-EGa): 49.3%, 23.5%, 6.1%, 17.6%, 3.5%.

3.3. Surface Composition after Immersion in Water

In order to evaluate the response of the amphiphilic PDMS-based films to the water environment, an AR-XPS analysis was also carried out on the films after immersion in water for 7 days. The chemical composition of these film surfaces is however indicative of the actual composition as it represents a kinetically trapped condition and not the equilibrium state reached by the polymer surface upon immersion in water. The atomic compositions of the surfaces after water immersion are collected in Table 4. Generally, the film surfaces were highly enriched in fluorine with respect to the theoretical amount and its percent content decreased with decreasing φ , thus showing that a composition gradient was maintained upon contact with water. On the other hand, the atomic percentages of all the other elements were lower than the theoretical ones and increased with decreasing φ . However, the chemical composition of the film surface as well as its modification upon immersion in water strictly depended on the type of terpolymer introduced in the formulation. In particular, the films containing p(Sib-F-EGb) underwent a surface reconstruction after immersion which resulted in a significant surface depletion in F moieties and enrichment in Si and O. A similar trend, although less marked, was observed for the film p(Sib-F-EGa)4, while the film p(Sia-F-EGa)4 did not display a significant variation in the atomic percentages and only showed a slight increase in F upon immersion in water. Consistently, the C(1s) signal of p(Sia-F-EGa)4 after immersion almost exactly overlapped the corresponding signal before immersion, with a slight increase in the intensity of the peaks (iv) and (v) due to the CF₂ and CF₃ groups (Figure 4c). For p(Sib-F-EGa)4 the C(1s) signals before and after immersion were very similar, with a slight increase in the intensity of peak (i) associated with the C–Si contribution (Figure 4a). However, in neither case was an increase in the C–O contribution (peak (ii)) detected, indicating that the amount of EG as well as F chains remained practically unchanged after immersion in water.

Table 4. XPS atomic surface composition of the amphiphilic PDMS-based films p(Si-F-EG)4 after 7 days of immersion in water. The errors on the values of composition were estimated to be $\pm 0.5\%$.

Film	φ (°)	C (%)	O (%)	F (%)	Si (%)	$C_{\text{exp}}/C_{\text{theor}}$	$O_{\text{exp}}/O_{\text{theor}}$	$F_{\text{exp}}/F_{\text{theor}}$	$Si_{\text{exp}}/Si_{\text{theor}}$
p(Sib-F-EGa)4	theor.	50.0	24.9	~0.4	24.7				
	70	43.4	14.7	34.3	7.6	0.9	0.6	85.7	0.3
	20	47.8	20.0	19.9	12.3	1.0	0.8	49.7	0.5
p(Sib-F-EGb)4	theor.	50.2	25.0	~0.2	24.6				
	70	45.0	21.7	21.6	11.7	0.9	0.9	108.0	0.5
	20	48.9	24.6	11.2	15.3	1.0	1.0	56.0	0.6
p(Sia-F-EGa)4	theor.	50.1	24.6	1.1	24.2				
	70	40.3	10.2	47.3	2.2	0.8	0.4	43.0	0.1
	20	43.5	12.6	40.5	3.4	0.9	0.5	36.8	0.1

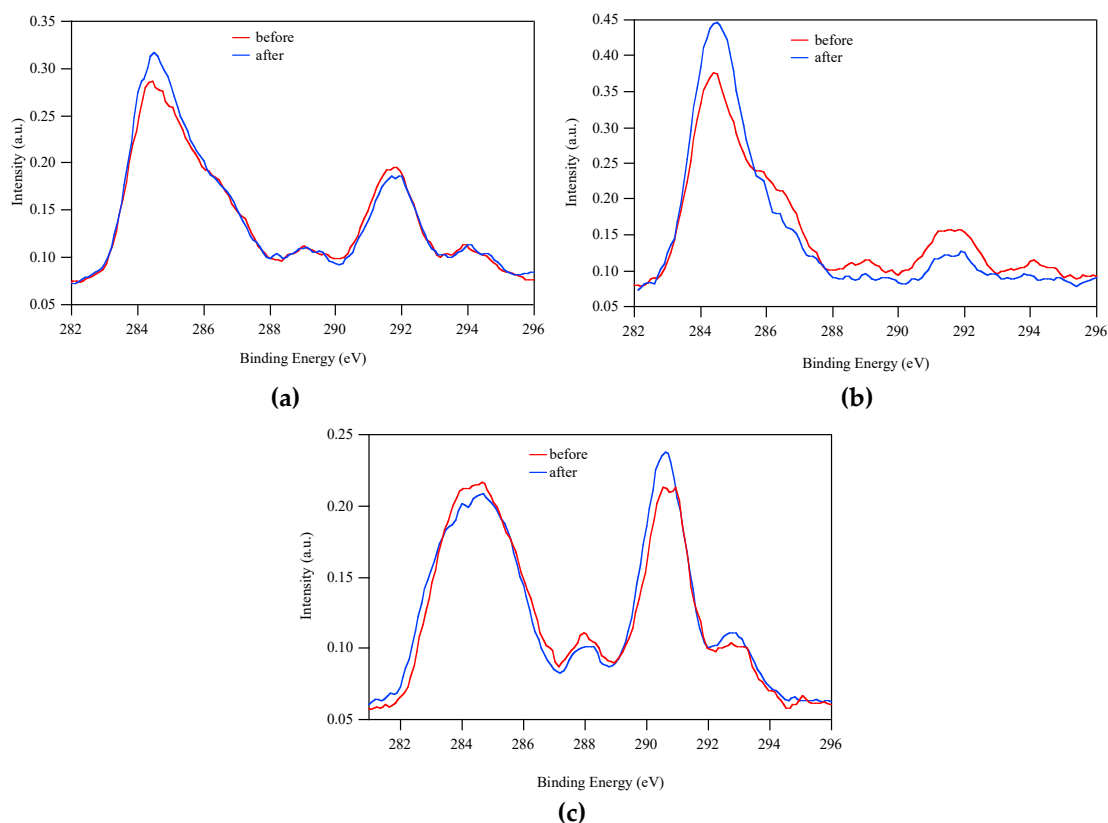


Figure 4. Area-normalized C(1s) XPS spectra ($\varphi = 70^\circ$) for p(Sib-F-EGa)4 (a), p(Sib-F-EGb)4 (b) and p(Sia-F-EGa)4 (c) before (red) and after (blue) immersion in water.

The comparison of C(1s) signals before and after immersion for p(Sib-F-EGb)4 revealed the presence of significant differences, indicating that these films were subjected to a massive surface reconstruction as a result of the combination of Sib, EGb and F chains in the same chemical structure. The intensities of the peaks due to CF_3 , CF_2 and $C(=O)O$ moieties markedly decreased, while that associated with $C-Si$ increased (Figure 4b). Unexpectedly, the intensity of the signal due to the $C-O$ groups of the longer EGb chains decreased upon immersion in water (Figure 4b). However, the $C-O/(CF_2 + CF_3)$ ratio increased (Table 5), indicating that the hydrophilic/hydrophobic balance, i.e. the amphiphilic character, of the film surface was larger after immersion.

Table 5. Percent contributions of peaks (i)–(v) to the XPS C(1s) signal for the amphiphilic PDMS-based films ($\varphi = 70^\circ$) after immersion in water for 7 days.

Film	Peak (i) (%)	Peak (ii) (%)	Peak (iii) (%)	Peak (iv) (%)	Peak (v) (%)
p(Sib-F-EGa)4	33.7	30.4	4.6	24.6	6.7
p(Sib-F-EGb)4	66.7	27.1	-	6.2	-
p(Sia-F-EGa)4	13.2	38.3	4.2	37.3	7.0

Overall, it appears that, when F and EGa were combined in the same macromolecular structure, the maximum concentration of the EG chains at the outermost surface (*cf.* C(1s) signal percentages at $\varphi = 70^\circ$ and 20° for p(Sib-F-EGa)4 and p(Sia-F-EGa)4) did not provide the necessary driving force for reconstruction, resulting in a chemical stability of the surface upon contact with water at least for the investigated time of 7 days. A very different process occurred when F and EGb were combined instead. A greater accumulation of the longer EGb chains in a region immediately below the outer surface (*cf.* C(1s) signal percentages at $\varphi = 70^\circ$ and 20° for p(Sib-F-EGb)4) provided the right drive for surface reconstruction, resulting from the tendency of the EG chains to migrate to contact water. Actually, a reconstruction mechanism appears mainly to involve the migration of the hydrophobic fluorinated chains away from the polymer–water interface, rather than the migration of the hydrophilic ethoxylated chains toward the surface, as suggested by the reduction in the amount of C–O groups after immersion in water. This was possibly due to the effect of the concomitant presence of F chains that mechanically dragged part of the EG chains into the film bulk, thus preventing the effective migration of the latter to the polymer–water interface. However, the decrease in the F chains was much more marked than that in the EG ones, resulting in an increased C–O/(CF₂ + CF₃) ratio and consistently in a higher hydrophilicity of the whole system. This peculiar reconstruction mechanism differs from that generally reported for other amphiphilic copolymers containing ethoxylated and fluorinated components, which led to a substantial increase in surface concentration of the ethoxylated chains as a result of their major exposure to water [47–50].

In agreement with these last conclusions, measurements of static contact angle with water (θ_w) at different immersion times in water up to 6 days showed that θ_w decreased from $113^\circ \pm 2$, $111^\circ \pm 2$ and $106^\circ \pm 2$ to $106^\circ \pm 2$, $106^\circ \pm 2$ and $84^\circ \pm 2$ for p(Sib-F-EGa)4, p(Sia-F-EGa)4 and p(Sib-F-EGb)4, respectively. The last film surfaces underwent a more pronounced reconstruction becoming more hydrophilic after contact with water. Atomic force microscopy (AFM) measurements showed that all film surfaces were featureless and very smooth (RMS ~ 7 nm ($1 \times 1 \mu\text{m}^2$)). Therefore, the effect of surface roughness on θ_w could be neglected.

4. Concluding Remarks

Novel surface-active amphiphilic terpolymers composed of a (meth)acrylic backbone with fluorinated (F), ethoxylated (EG) and siloxane (Si) side chains were engineered with variable lengths of EG and Si chains for one given length of F chains to create chemically modified PDMS-based film surfaces within the outermost few nanometers. AR-XPS analysis proved that all the PDMS-based films containing the terpolymer displayed a surface chemical composition close to that of the respective parent terpolymer, indicating that the presence of the PDMS matrix as the major component in the formulation did not inhibit the strong surface segregation of the terpolymer, which was responsible for the exceptionally high enrichment in fluorine of the outermost surface layers with respect to the bulk of the film. Even though the experimental amount of fluorine at the surface was lower for the sample p(Sib-F-EGb)4 consisting of both longer siloxane and ethoxylated side chains, the $F_{\text{exp}}/F_{\text{theor}}$ ratio was the highest, indicating that the surface segregation process was the most effective for this terpolymer. The substantial surface segregation of the fluorinated chains produced an accumulation of the high surface energy ethoxylated chains at the polymer–air interface, thus resulting in an amphiphilic, chemically heterogeneous surface structure at the nanoscale level of the otherwise hydrophobic siloxane surface. In particular, the concentration of CH₂CH₂O groups within the first ~ 3 nm of

the polymer surface was maximized for terpolymers containing the shorter and more mobile EGa side chains.

The sensitivity of the polymer films to the water environment depended on the structure of the terpolymer and in particular on the length of the EG side chains and their content at the polymer–air interface. In fact, for films p(Sia-F-EGa)₄ and p(Sib-F-EGa)₄, with the maximum percentage of CH₂CH₂O groups at the outermost surface layers ($\varphi = 70^\circ$), the C–O/(CF₃ + CF₂) ratio, namely an estimation of the hydrophilic/hydrophobic balance of the system, did not change upon immersion in water, since the chemistry of the film surface was stable upon immersion. On the other hand, for films of p(Sib-F-EGb)₄, with a higher content of CH₂CH₂O groups in the bulk ($\varphi = 20^\circ$), the C–O/(CF₃ + CF₂) significantly increased showing that the film surface became more hydrophilic upon immersion in water. However, in no case was an enhancement detected in ethoxylated chain concentration at the surface after immersion. The reconstruction process involved a massive migration of the fluorinated tails away from the surface, which led to a marked increase in the amphiphilicity degree, although part of the ethoxylated chains were also concurrently dragged into the bulk.

The features of surface structure and reconstruction of amphiphilic polymer coatings are highly relevant to potential application, notably when distinct interactions with the water environment are involved. Simultaneous incorporation of opposite, hydrophobic and hydrophilic, functions into a surface-active terpolymer-based coating leads to a chemically heterogeneous and dynamically rearranging coating surface. Such coating is conceivably able to better resist adhesion from diverse fouling agents, such as bacteria, cells and organisms, especially those that exhibit contrasting preferences for hydrophilic, or otherwise hydrophobic, surface characters. One prime example is in the field of marine antifouling/fouling-release coating application.

Supplementary Materials: The following are available online at <http://www.mdpi.com/2079-6412/9/3/153/s1>, Figure S1: Differential scanning calorimetry (DSC) heating curves of the amphiphilic terpolymers p(Sib-F-EGa) and p(Sib-F-EGb). Figure S2: Area-normalized C(1s) XPS spectra of p(Sib-F-EGa)₄ (a), p(Sib-F-EGb)₄ (b) and p(Sia-F-EGa)₄ (c).

Author Contributions: Conceptualization, G.G., E.G. and E.M.; methodology, G.G.; software, E.G. and A.G.; validation, E.M., E.G. and A.G.; formal analysis, E.M.; investigation, E.M., E.G. and A.G.; resources, G.G.; data curation, E.M. and E.G.; writing—original draft preparation, E.M.; writing—review and editing, G.G.; visualization, E.G.; supervision, G.G.; project administration, G.G. and E.M.; funding acquisition, G.G.

Funding: This research was funded by support from the University of Pisa (Progetti di Ricerca di Ateneo, PRA_2017_17).

Conflicts of Interest: The authors declare no conflict of interest.

References

1. Narrainen, A.P.; Hutchings, L.R.; Ansari, I.; Thompson, R.L.; Clarke, N. Multi-End-Functionalized polymers: Additives to modify polymer properties at surfaces and interfaces. *Macromolecules* **2007**, *40*, 1969–1980. [[CrossRef](#)]
2. Lee, H.; Archer, L.A. Functionalizing polymer surfaces by surface migration of copolymer additives: Role of additive molecular weight. *Polymer* **2002**, *43*, 2721–2728. [[CrossRef](#)]
3. Martinelli, E.; Galli, G.; Cwikel, D.; Murmur, A. Wettability and surface tension of amphiphilic polymer films: time-dependent measurements of the most stable contact angle. *Macromol. Chem. Phys.* **2012**, *213*, 1448–1456. [[CrossRef](#)]
4. Yasani, B.R.; Martinelli, E.; Galli, G.; Glisenti, A.; Mieszkin, S.; Callow, M.E.; Callow, J.A. A comparison between different fouling-release elastomer coatings containing surface-active polymers. *Biofouling* **2014**, *30*, 387–399. [[CrossRef](#)] [[PubMed](#)]
5. Lee, H.; Archer, L.A. Functionalizing polymer surfaces by field-induced migration of copolymer additives. 1. Role of surface energy gradients. *Macromolecules* **2001**, *34*, 4572–4579. [[CrossRef](#)]
6. Martinelli, E.; Fantoni, C.; Galli, G.; Gallot, B.; Glisenti, A. Low surface energy properties of smectic fluorinated block copolymer/SEBS blends. *Mol. Cryst. Liq. Cryst.* **2009**, *500*, 51–62. [[CrossRef](#)]

7. Inutsuka, M.; Yamada, N.L.; Ito, K.; Yokoyama, H. High density polymer brush spontaneously formed by the segregation of amphiphilic diblock copolymers to the polymer/water interface. *ACS Macro Lett.* **2013**, *2*, 265–268. [[CrossRef](#)]
8. Martinelli, E.; Hill, S.D.; Finlay, J.A.; Callow, M.E.; Callow, J.A.; Glisenti, A.; Galli, G. Amphiphilic modified-styrene copolymer films: antifouling/fouling release properties against the green alga *Ulva linza*. *Prog. Org. Coat.* **2016**, *90*, 235–242. [[CrossRef](#)]
9. Mielczarski, J.; Mielczarski, E.; Galli, G.; Morelli, A.; Martinelli, E.; Chiellini, E. The surface-segregated nanostructure of fluorinated copolymer-poly(dimethylsiloxane) blend films. *Langmuir* **2010**, *26*, 2871–2876. [[CrossRef](#)] [[PubMed](#)]
10. Sorgi, C.; Martinelli, E.; Galli, G.; Pucci, A. Julolidine-labelled fluorinated block copolymers for the development of two-layer films with highly sensitive vapochromic response. *Sci. China Chem.* **2018**, *61*, 947–956. [[CrossRef](#)]
11. Raffa, P.; Wever, D.A.Z.; Picchioni, F.; Broekhuis, A.A. Polymeric surfactants: Synthesis, properties, and links to applications. *Chem. Rev.* **2015**, *115*, 8504–8563. [[CrossRef](#)] [[PubMed](#)]
12. Galli, G.; Martinelli, E. Amphiphilic polymer platforms: Surface engineering of films for marine antibiofouling. *Macromol. Rapid Commun.* **2017**, *38*. [[CrossRef](#)] [[PubMed](#)]
13. Martin, C.; Aibani, N.; Callan, J.F.; Callan, B. Recent advances in amphiphilic polymers for simultaneous delivery of hydrophobic and hydrophilic drugs. *Ther. Deliv.* **2016**, *7*, 15–31. [[CrossRef](#)] [[PubMed](#)]
14. Nesvadba, P. Radical polymerization in industry. In *The Encyclopedia of Radicals in Chemistry, Biology and Materials*; John Wiley & Sons: Hoboken, NJ, USA, 2012.
15. Li, L.; Raghupathi, K.; Song, C.; Prasada, P.; Thayumanavan, S. Self-assembly of random copolymers. *Chem. Commun.* **2014**, *50*, 13417–13432. [[CrossRef](#)] [[PubMed](#)]
16. Matsumoto, K.; Terashima, T.; Sugita, T.; Takenaka, M.; Sawamoto, M. Amphiphilic random copolymers with hydrophobic/hydrogen-bonding urea pendants: Self-folding polymers in aqueous and organic media. *Macromolecules* **2016**, *49*, 7917–7927. [[CrossRef](#)]
17. Terashima, T.; Sugita, T.; Fukae, K.; Sawamoto, M. Synthesis and single-chain folding of amphiphilic random copolymers in water. *Macromolecules* **2014**, *47*, 589–600. [[CrossRef](#)]
18. Koda, Y.; Terashima, T.; Sawamoto, M. Multimode self-folding polymers via reversible and thermoresponsive self-assembly of amphiphilic/fluorous random copolymers. *Macromolecules* **2016**, *49*, 4534–4543. [[CrossRef](#)]
19. Guazzelli, E.; Masotti, E.; Biver, T.; Pucci, A.; Martinelli, E.; Galli, G. The self-assembly over nano- to submicro-length scales in water of a fluorescent julolidine-labeled amphiphilic random terpolymer. *J. Polym. Sci. Part A Polym. Chem.* **2018**, *56*, 797–804. [[CrossRef](#)]
20. Martinelli, E.; Guazzelli, E.; Galli, G.; Telling, M.T.F.; Dal Poggetto, G.; Immirzi, B.; Domenici, F.; Paradossi, G. Prolate and temperature-responsive self-assemblies of amphiphilic random copolymers with perfluoroalkyl and polyoxyethylene side chains in solution. *Macromol. Chem. Phys.* **2018**, *219*, 1800210. [[CrossRef](#)]
21. Galli, G.; Barsi, D.; Martinelli, E.; Glisenti, A.; Finlay, J.A.; Callow, M.E.; Callow, J.A. Copolymer films containing amphiphilic side chains of well-defined fluoroalkyl-segment length with biofouling-release potential. *RSC Adv.* **2016**, *6*, 67127–67135. [[CrossRef](#)]
22. Rufin, M.A.; Ngo, B.K.D.; Barry, M.E.; Page, V.M.; Hawkins, M.L.; Stafslie, S.J.; Grunlan, M.A. Antifouling silicones based on surface-modifying additive amphiphiles. *Green Mater.* **2017**, *5*, 4–13. [[CrossRef](#)]
23. Stafslie, S.J.; Christianson, D.; Daniels, J.; VanderWal, L.; Chernykha, A.; Chisholm, B.J. Combinatorial materials research applied to the development of new surface coatings XVI: Fouling-release properties of amphiphilic polysiloxane coatings. *Biofouling* **2015**, *31*, 135–149. [[CrossRef](#)] [[PubMed](#)]
24. Martinelli, E.; Del Moro, I.; Galli, G.; Barbaglia, M.; Bibbiani, C.; Mennillo, E.; Oliva, M.; Pretti, C.; Antonioli, D.; Laus, M. Photopolymerized network polysiloxane films with dangling hydrophilic/hydrophobic chains for the biofouling release of invasive marine serpulid *Ficopomatus enigmaticus*. *ACS Appl. Mater. Interfaces* **2015**, *7*, 8293–8301. [[CrossRef](#)] [[PubMed](#)]
25. Martinelli, E.; Pretti, C.; Oliva, M.; Glisenti, A.; Galli, G. Sol-gel polysiloxane films containing different surface-active trialkoxysilanes for the release of the marine foulant *Ficopomatus enigmaticus*. *Polymer* **2018**, *145*, 426–433. [[CrossRef](#)]
26. Noguer, A.C.; Olsen, S.M.; Hvilsted, S.; Kiil, S. Diffusion of surface-active amphiphiles in silicone-based fouling-release coatings. *Prog. Org. Coat.* **2017**, *106*, 77–86. [[CrossRef](#)]

27. Martinelli, E.; Gunes, D.; Wenning, B.M.; Ober, C.K.; Finlay, J.A.; Callow, M.E.; Callow, J.A.; Di Fino, A.; Clare, A.S.; Galli, G. Effects of surface-active block copolymers with oxyethylene and fluoroalkyl side chains on the antifouling performance of silicone-based film. *Biofouling* **2016**, *32*, 81–93. [[CrossRef](#)] [[PubMed](#)]
28. Patterson, A.L.; Wenning, B.; Rizis, G.; Calabrese, D.R.; Finlay, J.A.; Franco, S.C.; Zuckermann, R.N.; Clare, A.S.; Kramer, E.J.; Ober, C.K.; et al. Role of backbone chemistry and monomer sequence in amphiphilic oligopeptide- and oligopeptoid-functionalized PDMS- and PEO-based block copolymers for marine antifouling and fouling release coatings. *Macromolecules* **2017**, *50*, 2656–2667. [[CrossRef](#)]
29. Weinman, C.J.; Finlay, J.A.; Park, D.; Paik, M.Y.; Krishnan, S.; Sundaram, H.S.; Dimitriou, M.; Sohn, K.E.; Callow, M.E.; Callow, J.A.; et al. ABC triblock surface active block copolymer with grafted ethoxylated fluoroalkyl amphiphilic side chains for marine antifouling/fouling-release applications. *Langmuir* **2009**, *25*, 12266–12274. [[CrossRef](#)] [[PubMed](#)]
30. Gombotz, W.R.; Guanghai, W.; Horbett, T.A.; Hoffman, A.S. Protein adsorption to poly(ethylene oxide) surfaces. *J. Biomed. Mater. Res.* **1991**, *25*, 1547–1562. [[CrossRef](#)] [[PubMed](#)]
31. Krishnan, S.; Weinman, C.J.; Ober, C.K. Advances in polymers for anti-biofouling surfaces. *J. Mater. Chem.* **2008**, *18*, 3405–3413. [[CrossRef](#)]
32. Brady, R.F. Foul-release coatings for warships. *Def. Sci. J.* **2005**, *55*, 75–81. [[CrossRef](#)]
33. Lejars, M.; Marigaillan, A.; Bressy, C. Foul release coatings: A nontoxic alternative to biocidal antifouling coatings. *Chem. Rev.* **2012**, *112*, 4347–4390. [[CrossRef](#)] [[PubMed](#)]
34. Krishnan, S.; Wang, N.; Ober, C.K.; Finlay, J.A.; Callow, M.E.; Callow, J.A.; Hexemer, A.; Sohn, K.E.; Kramer, E.J.; Fischer, D.A. Comparison of the fouling release properties of hydrophobic fluorinated and hydrophilic PEGylated block copolymer surfaces: Attachment strength of the diatom *Navicula* and the green alga *Ulva*. *Biomacromolecules* **2006**, *7*, 1449–1462. [[CrossRef](#)] [[PubMed](#)]
35. Galli, G.; Martinelli, E.; Chiellini, E.; Ober, C.K.; Glisenti, A. Low surface energy characteristics of mesophase forming ABC, ACB triblock copolymers with fluorinated B blocks. *Mol. Cryst. Liq. Cryst.* **2005**, *441*, 211–226. [[CrossRef](#)]
36. Martinelli, E.; Galli, G.; Krishnan, S.; Paik, M.Y.; Ober, C.K.; Fischer, D.A. New poly(dimethylsiloxane)/poly(perfluorooctylethyl acrylate) block copolymers: Structure and order across multiple length scales in thin films. *J. Mater. Chem.* **2011**, *21*, 15357–15368. [[CrossRef](#)]
37. Wenning, B.M.; Martinelli, E.; Mieszkina, S.; Finlay, J.A.; Fischer, D.; Callow, J.A.; Callow, M.E.; Leonardi, A.K.; Ober, C.K.; Galli, G. Model amphiphilic block copolymers with tailored molecular weight and composition in PDMS-based films to limit soft biofouling. *ACS Appl. Mater. Interfaces* **2017**, *9*, 16505–16516. [[CrossRef](#)] [[PubMed](#)]
38. Martinelli, E.; Glisenti, A.; Gallot, B.; Galli, G. Surface properties of mesophase-forming fluorinated bicycloacrylate/polysiloxane methacrylate copolymers. *Macromol. Chem. Phys.* **2009**, *210*, 1746–1753. [[CrossRef](#)]
39. Sundaram, H.S.; Cho, Y.; Dimitriou, M.D.; Weinman, C.J.; Finlay, J.A.; Cone, G.; Callow, M.E.; Callow, J.A.; Kramer, E.J.; Ober, C.K. Fluorine-free mixed amphiphilic polymers based on PDMS and PEG side chains for fouling release applications. *Biofouling* **2011**, *27*, 589–602. [[CrossRef](#)] [[PubMed](#)]
40. Majumdar, P.; Stafslie, S.; Daniels, J.; Webster, D.C. High throughput combinatorial characterization of thermosetting siloxane-urethane coatings having spontaneously formed microtopographical surfaces. *J. Coat. Technol. Res.* **2007**, *4*, 131–138. [[CrossRef](#)]
41. Bodkhe, R.B.; Stafslie, S.J.; Cilz, N.; Daniels, J.; Thompson, S.E.M.; Callow, M.E.; Callow, J.A.; Webster, D.C. Polyurethanes with amphiphilic surfaces made using telechelic functional PDMS having orthogonal acid functional groups. *Prog. Org. Coat.* **2012**, *75*, 38–48. [[CrossRef](#)]
42. Martinelli, E.; Guazzelli, E.; Galli, G. Recent advances in designed non-toxic polysiloxane coatings to combat marine biofouling. In *Marine Coatings and Membranes*; Mittal, V., Ed.; Central West Publishing: Orange, NSW, Australia, 2019.
43. Shirley, D.A. High-resolution X-ray photoemission spectrum of the valence bands of gold. *Phys. Rev. B* **1972**, *5*, 4709. [[CrossRef](#)]
44. Moulder, J.F.; Stickle, W.F.; Sobol, P.E.; Bomben, K.D. *Handbook of X-ray Photoelectron Spectroscopy, Physical Electronics*; Perkin-Elmer Corp.: Eden Prairie, MN, USA, 1992.
45. McIntyre, N.S.; Chan, T.C. *Practical Surface Analysis 1*; Briggs, D., Seah, M.P., Eds.; Wiley: Chichester, UK, 1990; p. 485.

46. Marabotti, I.; Morelli, A.; Orsini, L.M.; Martinelli, E.; Galli, G.; Chiellini, E.; Lien, E.M.; Pettitt, M.E.; Callow, M.E.; Callow, J.A.; et al. Fluorinated/siloxane copolymer blends for fouling release: Chemical characterisation and biological evaluation with algae and barnacles. *Biofouling* **2009**, *25*, 481–493. [[CrossRef](#)] [[PubMed](#)]
47. Gudipati, C.S.; Greenleaf, C.M.; Johnson, J.A.; Pryoncpn, P.; Wooley, K.L. Hyperbranched fluoropolymer and linear poly(ethylene glycol) based amphiphilic crosslinked networks as efficient antifouling coatings: An insight into the surface compositions, topographies, and morphologies. *J. Polym. Sci. Part A Polym. Chem.* **2004**, *42*, 6193–6208. [[CrossRef](#)]
48. Krishnan, S.; Ayothi, R.; Hexemer, A.; Finlay, J.A.; Sohn, K.E.; Perry, R.; Ober, C.K.; Kramer, E.J.; Callow, M.E.; Callow, J.A.; et al. Anti-biofouling properties of comblike block copolymers with amphiphilic side chains. *Langmuir* **2006**, *22*, 5075–5086. [[CrossRef](#)] [[PubMed](#)]
49. Krishnan, S.; Paik, M.Y.; Ober, C.K.; Martinelli, E.; Galli, G.; Sohn, K.E.; Kramer, E.J.; Fischer, D.A. NEXAFS depth profiling of surface segregation in block copolymer thin films. *Macromolecules* **2010**, *43*, 4733–4743. [[CrossRef](#)]
50. Martinelli, E.; Pelusio, G.; Yasani, B.R.; Glisenti, A.; Galli, G. Surface chemistry of amphiphilic polysiloxane/triethyleneglycol-modified poly(pentafluorostyrene) block copolymer films before and after water immersion. *Macromol. Chem. Phys.* **2015**, *216*, 2086–2094. [[CrossRef](#)]



© 2019 by the authors. Licensee MDPI, Basel, Switzerland. This article is an open access article distributed under the terms and conditions of the Creative Commons Attribution (CC BY) license (<http://creativecommons.org/licenses/by/4.0/>).